

Solid-State Aggregation of Metallacyclophane-Based Mn^{II}Cu^{II} One-Dimensional Ladders

Jesús Ferrando-Soria,[†] Thais Grancha,[†] Jorge Pasán,[‡] Catalina Ruiz-Pérez,[‡] Laura Cañadillas-Delgado,[§] Yves Journaux,[⊥] Miguel Julve,[‡] Joan Cano,[‡] Francesc Lloret,^{*‡} and Emilio Pardo^{*‡}

[†]Departament de Química Inorgànica, Instituto de Ciencia Molecular (ICMOL), Universitat de València, 46980 Paterna, València, Spain

[‡]Laboratorio de Rayos X y Materiales Moleculares, Departamento de Física Fundamental II, Universidad de La Laguna, 38201 La Laguna, Tenerife, Spain

[§]Institut Laue Langevin, 38042 Grenoble, France

[⊥]Institut Parisien de Chimie Moléculaire, Université Pierre et Marie Curie-Paris 6, UMR 7201, F-75252 Paris, France

Supporting Information

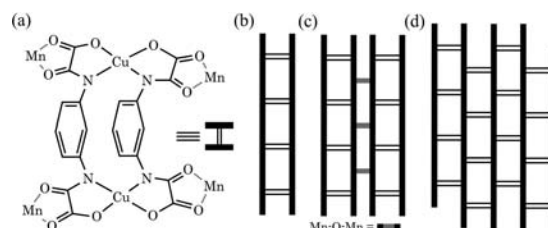
ABSTRACT: Two distinct one-dimensional (1) and two-dimensional (2) mixed-metal–organic polymers have been synthesized by using the “complex-as-ligand” strategy. The structure of 1 consists of isolated ladderlike Mn^{II}Cu^{II}₂ chains separated from each other by neutral Mn^{II}₂ dimers, whereas 2 possesses an overall corrugated layer structure built from additional coordinative interactions between adjacent Mn^{II}Cu^{II}₂ ladders. Interestingly, 1 and 2 show overall ferri- and antiferromagnetic behavior, respectively, as a result of their distinct crystalline aggregation in the solid state.

The design and synthesis of metal–organic polymers (MOPs)¹ with interesting and predictable magnetic properties has been a subject of great interest for inorganic chemists interested in molecular magnetism during the last 3 decades.^{2–4} One- (1D), two- (2D), and three-dimensional (3D) MOPs are also relevant from a crystal-engineering point of view⁵ because of the wide range of structural motifs and intriguing topologies that can be found. In the search for rationally designed *n*D (*n* = 1–3) MOPs,^{1c,d} the molecular-programmed self-assembling methods show clear advantages over the so-called serendipitous self-assembling ones.^{1a,b} However, total control of the final structure is still a challenge even when following these rational synthetic strategies. In fact, there are many subtle factors that may affect the self-assembly process, both intrinsic (stereochemical and steric requirements of the metal and ligand, respectively) and extrinsic (metal–ligand ratio, solvent, and temperature),⁶ and then influence the final structure of the MOPs.

Our strategy in this field is based on the use of oxamate-based homodinuclear copper(II), nickel(II), and cobalt(II) metallacyclic complexes as ligands (metalloligands) toward fully solvated divalent first-row transition-metal ions like manganese(II) and cobalt(II) to afford mixed-metal–organic polymers, abbreviated as M'MOPs, of varying dimensionality.^{7,1c,d} So, for instance, the double-stranded dicopper(II) metallacyclophanes of the general formula [Cu₂L₂]^{4–} [L = *N,N'*-1,3-phenylenebis(oxamate) (mpba), 2-methyl-*N,N'*-1,3-phenylenebis(oxamate)

(Mempba), and 2,4,6-trimethyl-*N,N'*-1,3-phenylenebis(oxamate) (Me₃mpba)]⁷ can be advantageously used as a tetrakis(bidentate) metalloligand toward bis(chelated) M^{II} ions (M = Mn and Co) to render neutral M'MOPs with different 1D or 2D architectures (Scheme 1). In follow-up works,^{7a,b} some

Scheme 1. Self-Assembly of 1D (b) and 2D (c and d) M'MOPs Resulting from the Use of a Dicopper(II) Metallacyclophane Anion (a) as the Tetrakis(bidentate) Metalloligand toward Bis(chelated) Mn^{II} Ions



of us reported two examples of 2D M'MOPs possessing a “brick-wall” rectangular layer structure of (6, 3) net topology that were obtained through the self-assembly of the anionic dicopper(II) complexes [Cu₂(mpba)₂]^{4–} and [Cu₂(Me₃mpba)₂]^{4–} with Co^{II} or Mn^{II} ions, respectively (Scheme 1b).^{7a,b}

In this Communication, we show that 1D (1) and 2D (2) M'MOPs with a basic “ladderlike” structural motif but different degrees of aggregation in the solid state (Scheme 1b,c), can be alternatively obtained under different experimental conditions. Herein we report the syntheses, crystal structures, and magnetic properties of these new examples of M'MOPs of formulas [Mn₄(H₂mpba)₄(H₂O)₁₂]{[Mn₈Cu₈(mpba)₈(H₂O)₂₄]}·29.5H₂O (1) and [Mn₄Cu₄(mpba)₄(H₂O)₉].14H₂O (2).

Compounds 1 and 2 were both obtained as pale-green rectangular and cubic crystals, respectively, by slow diffusion in an H-shaped tube of aqueous solutions of Na₄[Cu₂(mpba)₂].8H₂O^{7a} and Mn(NO₃)₂.4H₂O at 16 °C.

Received: May 9, 2012

Published: June 18, 2012

Interestingly, control of the temperature is crucial to avoid formation of the MOP with the “brick-wall” structure.^{7a,b} Moreover, the dicopper(II) complex/manganese(II) molar ratio also plays a key role in the self-assembling process. Thus, a 2D network with a Cu/Mn ratio of 1:1 (**2**) crystallized when using the stoichiometric relation (1:2). However, when this molar ratio was increased to 1:6 in the double H-shaped tube, a double-chain 1D compound (**1**) results with a final Cu/Mn ratio of 2:3. Their crystal structures were solved by single-crystal X-ray diffraction using synchrotron radiation at the BM16 beamline in the ESRF. They crystallize in the $P2_1cn$ (**1**) and $P2_1/c$ (**2**) space groups.

Complex **1** consists of neutral oxamato-bridged double copper(II)/manganese(II) chains, $[\text{Mn}_2\text{Cu}_2(\text{mpba})_2(\text{H}_2\text{O})_6]$ (Figures 1a and S1a in the Supporting Information, SI),

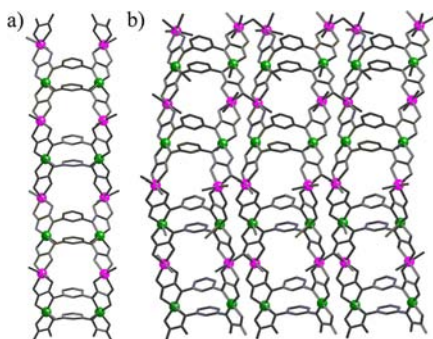


Figure 1. Perspective views of the fragments of two double chains of **1** (a) and the 2D neutral network of **2** (b). Metal and ligand atoms are represented by balls and sticks, respectively [Cu, green; Mn, purple].

cocrystallized $[\text{Mn}(\text{H}_2\text{mpba})(\text{H}_2\text{O})_3]$ chains, and free water molecules (Figure S1b in the SI). Each bis(oxamato)copper(II) entity acts as a bis(bidentate) ligand through the carbonyl oxygen atoms toward *cis*-diaquamanganese(II) units, affording zigzag double bimetallic chains that run parallel to the *c* axis (Figure 1a). These one-dimensional motifs possess a ladderlike architecture,^{7c,d} where two phenylenediamide bridges act as “rungs” between the two oxamate-bridged zigzag CuMn chains, which then serve as “rods”. The shortest intrachain Cu⋯Cu and Cu⋯Mn distances are in the ranges 6.654(2)–6.656(2) and 5.4532(14)–5.4865(15) Å, respectively.

The four crystallographically independent copper atoms in **1** [Cu(1)–Cu(4)] have five-coordinated square-pyramidal CuN_2O_3 surroundings, with two amide nitrogen atoms [Cu–N = 1.940(5)–2.061(6) Å] and two carboxylate oxygen atoms [Cu–O = 1.962(5)–2.052(4) Å] from the two oxamate ligands in a *trans* arrangement building the basal plane and the apical position being occupied by a water molecule [Cu–Ow = 2.322(5)–2.369(7) Å]. The four crystallographically independent manganese atoms of the double chains [Mn(1)–Mn(4)] are six-coordinate with two water molecules in *cis* positions [Mn–Ow = 2.096(6)–2.178(7) Å] and four oxygen atoms [Mn–O = 2.129(4)–2.258(7) Å] from two oxamate ligands, forming distorted octahedral surroundings.

In the crystal lattice of **1**, the zigzag CuMn double chains run along the [001] direction (Figure S2b in the SI). Moreover, they are displaced along the [010] direction, leading thus to an ABAB disposition pattern in the *ab* plane. Overall, this situation leads to large channels along the *c* axis that are occupied by the cocrystallized $[\text{Mn}(\text{H}_2\text{mpba})(\text{H}_2\text{O})_3]$ chains that situate perpendicularly to the CuMn double chains (Figure S2 in the

SI). Interestingly, there is a regular alternation of these highly disordered enantiopure Mn^{II} chains of opposite chiralities (Δ and Λ) along the *b* axis. The shortest interchain Cu⋯Cu, Cu⋯Mn, and Mn⋯Mn distances are 8.327(2), 5.150(2), and 5.761(4) Å, respectively.

The structure of **2** consists of neutral oxamato-bridged copper(II)/manganese(II) 2D networks, $[\text{Mn}_4\text{Cu}_4(\text{mpba})_4(\text{H}_2\text{O})_9]$ (Figure 1b) and crystallization water molecules. It can be alternatively described as a series of Cu_2Mn_2 double chains linked by coordinative interactions, giving rise to a corrugated 2D network. Each double chain has the same ladderlike structure of **1**; however, two carbonyl oxygen atoms from the oxamato ligands, which are coordinated to manganese(II) ions along the zigzag chain [O(1) and O(16)], also coordinate to manganese(II) ions of a neighboring double chain, giving rise to the final layered 2D structure (Figure 1b). The intrachain Cu⋯Cu and Cu⋯Mn distances through the oxamate and *m*-phenylene bridges are within the ranges of 6.7954(14)–6.8461(14) and 5.3328(11)–5.5510(11) Å, respectively. Along the 2D network, the shortest interchain Mn⋯Mn distance is 4.0399(12) Å and the Mn–O–Mn angle varies in the range 122.43(15)–122.51(15)°.

There are four crystallographically independent copper atoms in **2**. Three of them [Cu(1), Cu(2), and Cu(4)] have five-coordinated square-pyramidal CuN_2O_3 surroundings (Figure S3a in the SI), with two amidate nitrogen atoms [Cu–N = 1.960(3)–1.984(3) Å] and two carboxylate oxygen atoms [Cu–O = 1.969(3)–2.018(3) Å] from the oxamate groups of the ligands building the basal plane and the apical positions being occupied by a water molecule [Cu–Ow = 2.360(3)–2.600(4) Å]. The fourth copper atom [Cu(3)] has a square-planar CuN_2O_3 environment [Cu–N = 1.956(3)–1.965(3) Å and Cu–O = 1.956(3)–1.978(3) Å]. There are also four crystallographically independent manganese atoms [Mn(1)–Mn(4)] that exhibit very distorted octahedral geometries, MnO_6 , formed by four carbonyl oxygen atoms from two oxamate groups in all cases [Mn–O = 2.089(3)–2.397(3) Å] and two coordinated water molecules in *trans* and *cis* dispositions for Mn(1) and Mn(4), respectively [Mn–Ow = 2.127(3)–2.259(3) Å], and one coordinated water molecule and one carbonyl oxygen atom from the oxamate group of a neighboring double chain in *trans* and *cis* dispositions for Mn(2) and Mn(3), respectively [Mn–O = 2.249(3)–2.313(3) Å and Mn–Ow = 2.126(3)–2.278(4) Å]. This coordination mode is rare when looking at other similar oxamato-bridged copper(II)/metal(II) MOPs.^{1c,d,8}

In the crystal lattice of **2**, the corrugated layers are slightly shifted from the neighboring ones, avoiding a perfect stacking along the *c* axis (Figure S3b in the SI). The shortest Cu–Cu, Cu–Mn, and Mn–Mn interlayer separations are 5.9958(11), 4.5757(10), and 5.1642(11) Å, respectively. In addition, intermolecular hydrogen bonds [Ow⋯Ow = 2.668(5)–3.112(8) Å] involving coordinated [either to manganese(II) and to copper(II) atoms] and crystallization water molecules build a three-dimensional motif (Figure S3b in the SI).

The magnetic properties of **1** and **2** in the form of $\chi_{\text{M}}T$ versus *T* plots [with χ_{M} being the molar magnetic susceptibility per Cu_2Mn_2 (**1**) and Cu_2Mn_2 (**2**) units] are very different (Figure 2). At room temperature, $\chi_{\text{M}}T$ values for **1** and **2** (12.46 and 9.03 $\text{cm}^3 \text{K mol}^{-1}$, respectively) are slightly lower than those expected for the sum of two square/square-pyramidal copper(II) ions (**1** and **2**) and three (**1**) or two (**2**) octahedral manganese(II) ions [$\chi_{\text{M}}T = 13.91$ (**1**) and 9.54 (**2**) $\text{cm}^3 \text{mol}^{-1}$

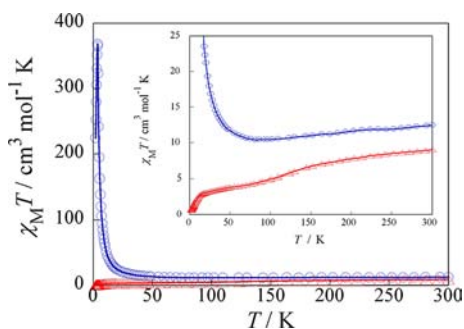


Figure 2. Temperature dependence of $\chi_M T$ of **1** (O, blue) and **2** (Δ , red) [under an applied magnetic field of 1 T ($T \geq 50$ K) and 250 G ($T < 50$ K)]. The inset shows in detail the different behavior of **1** and **2**. The solid lines are eye guides.

K with $g_{Mn} = 2.0$, $g_{Cu} = 2.1$, $S_{Mn} = 5/2$, and $S_{Cu} = 1/2$]. Upon cooling, $\chi_M T$ for **1** decreases, attains a minimum around 95 K (inset of Figure 2), and then rapidly increases to reach a maximum at about 4.0 K with $\chi_M T = 375$ cm³ K mol⁻¹ because of saturation effects. The presence of a minimum of $\chi_M T$ for **1** is characteristic of an overall ferrimagnetic behavior, as was previously observed in related oxamato-bridged manganese(II)/copper(II) chains.⁸ More likely, the moderate ferromagnetic interaction between copper(II) ions through the double *m*-phenylene bridge that occurs by means of a spin-polarization mechanism^{7c,d} is masked by the more important antiferromagnetic interaction between copper(II) and manganese(II) ions through the oxamate bridge.

On the contrary, $\chi_M T$ for **2** continuously decreases upon cooling to reach an incipient plateau in the range 75–15 K and then rapidly decreases and almost vanishes at 2.0 K ($\chi_M T = 0.58$ cm³ K mol⁻¹; inset of Figure 2). This overall antiferromagnetic behavior results from the nonnegligible antiferromagnetic coupling between neighboring double chains through the monatomic carboxylate–oxo bridge.⁹ The observed plateau is thus a consequence of the two different competitive magnetic interactions mediated by the oxamate– and carboxylate–oxo bridges, respectively.

In conclusion, a binuclear copper(II) precursor complex has been used as the metalloligand toward manganese(II) ions to afford two new MⁿMOPs with a common ladderlike chain motif. Yet, their distinct crystalline aggregation in the solid state leads to dramatically different magnetic properties. Thus, **1** behaves as a ferrimagnetic double chain with moderately strong antiferromagnetic intrachain coupling between copper(II) and manganese(II) ions through the oxamato bridge. In contrast, the antiferromagnetic interchain interactions between neighboring ferrimagnetic double chains dominate in **2**, giving rise to a $S = 0$ ground spin state.

■ ASSOCIATED CONTENT

Supporting Information

X-ray data in CIF format, experimental preparation, analytical and spectroscopic characterization (1/2), and additional figures (Figures S1–S3). This material is available free of charge via the Internet at <http://pubs.acs.org>.

■ AUTHOR INFORMATION

Corresponding Author

*E-mail: Emilio.Pardo@uv.es (E.P.), Francisco.Lloret@uv.es (F.L.).

Notes

The authors declare no competing financial interest.

■ ACKNOWLEDGMENTS

This work was supported by the MICINN (Spain; Projects CTQ2010-15364, MAT2010-19681, DPI2010-21103-C04-03, CSD2007-00010, and CSD2006-00015), the Generalitat Valenciana (Spain; Projects PROMETEO/2009/108 and ISIC/2012/002), the ACIISI-Gobierno Autónomo de Canarias (Spain; Project PIL-2070901 and structuring project NANOMAC), and the MFR and CNRS (France). We also acknowledge the Long Term Project HS3902 of the ESFR, Grenoble, France, for the beamtime assigned. J.F.-S. thanks the Generalitat Valenciana for a doctoral grant. E.P. and J.P. thank the “Juan de la Cierva” (MICINN) and the structuring project NANOMAC, respectively, for postdoctoral contracts.

■ REFERENCES

- (1) (a) Batten, S. R.; Robson, R. *Angew. Chem., Int. Ed.* **1998**, *37*, 1460. (b) Maspoch, D.; Ruiz-Molina, D.; Veciana, J. *Chem. Soc. Rev.* **2007**, *36*, 770. (c) Pardo, E.; Ruiz-García, R.; Cano, J.; Ottenwaelder, X.; Lescouëzec, R.; Journaux, Y.; Lloret, F.; Julve, M. *Dalton Trans.* **2008**, 2780. (d) Dul, M.-C.; Pardo, E.; Lescouëzec, R.; Journaux, Y.; Ferrando-Soria, J.; Ruiz-García, R.; Cano, J.; Julve, M.; Lloret, F.; Cangussu, D.; Pereira, C. L. M.; Stumpf, H. O.; Pasán, J.; Ruiz-Pérez, C. *Coord. Chem. Rev.* **2010**, *254*, 2281.
- (2) Pilkington, M.; Decurtins, S. In *Comprehensive Coordination Chemistry II: From Biology to Nanotechnology*; McCleverty, J. A., Meyer, T. J., Eds.; Elsevier: Oxford, U.K., 2004; Vol. 7, p 177.
- (3) Verdaguer, M.; Bleuzen, A.; Marvaud, V.; Vaissermann, J.; Seuleiman, M.; Desplanches, C.; Sculler, A.; Train, C.; Garde, R.; Gelly, G.; Lomenech, C.; Rosenman, I.; Veillet, P.; Cartier, C.; Villain, F. *Coord. Chem. Rev.* **1999**, *190*, 1023.
- (4) (a) Kahn, O. *Struct. Bonding (Berlin)* **1987**, *68*, 89. (b) Kahn, O. *Acc. Chem. Res.* **2000**, *33*, 647.
- (5) (a) Lehn, J. M. *Supramolecular Chemistry: Concepts and Perspectives*; VCH: Weinheim, Germany, 1995. (b) Leininger, S.; Olenyuk, B.; Stang, P. J. *Chem. Rev.* **2000**, *100*, 853.
- (6) (a) Tabellion, F. M.; Seidel, S. R.; Ari, A. M.; Stang, P. J. *J. Am. Chem. Soc.* **2001**, *123*, 7740. (b) Janiak, C. *Dalton Trans.* **2003**, 2781. (c) Biradha, K.; Sarkar, M.; Rajput, L. *Chem. Commun.* **2006**, 4169.
- (7) (a) Pereira, C. L. M.; Pedroso, E. F.; Stumpf, H. O.; Novak, M. A.; Ricard, L.; Ruiz-García, R.; Rivière, E.; Journaux, Y. *Angew. Chem., Int. Ed.* **2004**, *43*, 956. (b) Ferrando-Soria, J.; Pasán, J.; Ruiz-Pérez, C.; Journaux, Y.; Julve, M.; Lloret, F.; Cano, J.; Pardo, E. *Inorg. Chem.* **2011**, *50*, 8694. (c) Pardo, E.; Bernot, K.; Julve, M.; Lloret, F.; Cano, J.; Ruiz-García, R.; Delgado, F. S.; Ruiz-Pérez, C.; Ottenwaelder, X.; Journaux, Y. *Inorg. Chem.* **2004**, *43*, 2768. (d) Pardo, E.; Ruiz-García, R.; Lloret, F.; Julve, M.; Cano, J.; Pasán, J.; Ruiz-Pérez, C.; Filali, Y.; Chamoreau, L. M.; Journaux, Y. *Inorg. Chem.* **2007**, *46*, 4504. (e) Pardo, E.; Ferrando-Soria, J.; Dul, M.-C.; Lescouëzec, R.; Journaux, Y.; Ruiz-García, R.; Cano, J.; Julve, M.; Lloret, F.; Cañadillas-Delgado, L.; Pasán, J.; Ruiz-Pérez, C. *Chem.—Eur. J.* **2010**, *16*, 12838.
- (8) (a) Pardo, E.; Ruiz-García, R.; Lloret, F.; Faus, J.; Julve, M.; Journaux, Y.; Novak, M. A.; Delgado, F. S.; Ruiz-Pérez, C. *Chem.—Eur. J.* **2007**, *13*, 2054. (b) Ferrando-Soria, J.; Pardo, E.; Ruiz-García, R.; Cano, J.; Lloret, F.; Julve, M.; Journaux, Y.; Pasán, J.; Ruiz-Pérez, C. *Chem.—Eur. J.* **2011**, *17*, 2176. (c) Ferrando-Soria, J.; Cangussu, D.; Eslava, M.; Journaux, Y.; Lescouëzec, R.; Julve, M.; Lloret, F.; Pasán, J.; Ruiz-Pérez, C.; Lhotel, E.; Paulsen, C.; Pardo, E. *Chem.—Eur. J.* **2011**, *17*, 12482.
- (9) Milios, C. J.; Kefalloniti, E.; Raptopoulou, C. P.; Terzis, A.; Escuer, A.; Vicente, R.; Perlepes, S. P. *Polyhedron* **2004**, *83*.